Mössbauer spectra of single-domain particles in a weak magnetic field

2008 J. Phys.: Condens. Matter 20 505201

(http://iopscience.iop.org/0953-8984/20/50/505201)

J. Phys.: Condens. Matter **20** (2008) 505201 (10pp) doi:10.1088/0953-8984/20/50/505201

Mössbauer spectra of single-domain particles in a weak magnetic field

M A Chuev

Institute of Physics and Technology, Russian Academy of Sciences, 117218 Moscow, Russia

E-mail: chuev@ftian.ru

Received 4 August 2008, in final form 16 October 2008
Published 7 November 2008
Online at stacks.iop.org/JPhysCM/20/505201

Abstract

A three-level stochastic model taking into account the magnetic anisotropy, precession and diffusion of uniform magnetization of single-domain particles is developed in order to describe the Mössbauer absorption spectra of an ensemble of magnetic nanoparticles in a weak magnetic field. In contrast to conventional approaches searching for a distribution of the hyperfine field at nuclei, this model allows one to take into consideration physical mechanisms of formation of the magnetic hyperfine structure within the magnetic dynamics inherent to such materials. A number of qualitative effects observed in experimental Mössbauer spectra taken on small magnetic particles even in zero magnetic field can be self-consistently explained within the model in terms of the mean-field interparticle interaction. In particular, this model predicts the appearance of ^{57}Fe magnetic sextets with a small hyperfine splitting slightly dependent on the particle size and temperature in a weak magnetic field and at high temperature, which look like effective 'doublets' of lines often observed in experimental spectra.

1. Introduction

The great interest of researchers in modern materials containing nano-sized magnetic particles or clusters is primarily due to the wide area of their application in the nanotechnology of magnetic and magneto-optic information-recording devices, ferrofluids, NMR tomography, chemical catalysis, color imaging devices, biotechnology, etc. For this reason, it is necessary to perform systematic investigations of the structural and magnetic properties of these materials by various methods in order to optimize the technology of their growth and to determine the fundamental characteristics of magnetism in an ensemble of magnetic nanoparticles. A number of techniques can be used to study magnetic properties of nanoparticles, among which one of the most informative is Mössbauer spectroscopy. The shapes of the temperature- and field-dependent Mössbauer spectra obviously supply one with a large amount of information about physical characteristics inherent to the systems studied. The only way to extract the rich information from the experimental data is to define a model of the magnetic dynamics in order to describe the whole set of experimental data [1–4].

In contrast to the conventional magnetization measurements which are carried out at lower frequencies, Mössbauer spectroscopy can reveal the magnetic dynamics of nanoparticles at higher frequencies because the particle size is so small that the relaxation time of the magnetic moment of each particle can fall in the characteristic nuclear time window (10^{-11}–10^{-6} s for ^{57}Fe nuclei) and superparamagnetic relaxation can be the decisive factor in realizing specific shapes of the absorption spectrum [3, 5–7]. However, the conventional magnetization curves are widely measured as a function of both temperature and magnetic field [8–16], which supply one with a lot of data on the non-equilibrium magnetism of nanoparticles [4, 17], while the Mössbauer spectra of fine magnetic particles are usually collected as a function of temperature only [18–23]. In rare cases, when the spectra are measured in a strong external magnetic field of several Tesla, which is comparable with the strength of the hyperfine field, H_{hf}, at the nucleus, one can roughly estimate only the average saturation magnetization of the sample as a whole [24–26]. Meanwhile, a substantial influence of weak magnetic fields (of about a kilooersted or less) on magnetic characteristics of small particles has been observed not only in magnetization curves [8–16], but also in the field-dependent shape of Mössbauer spectra measured long ago [27, 28]. Moreover, the Mössbauer spectra of modern nanostructured magnetic alloys display a diverse transformation of their shapes in a radiofrequency magnetic field with an amplitude of about only ten oersteds [29, 30].

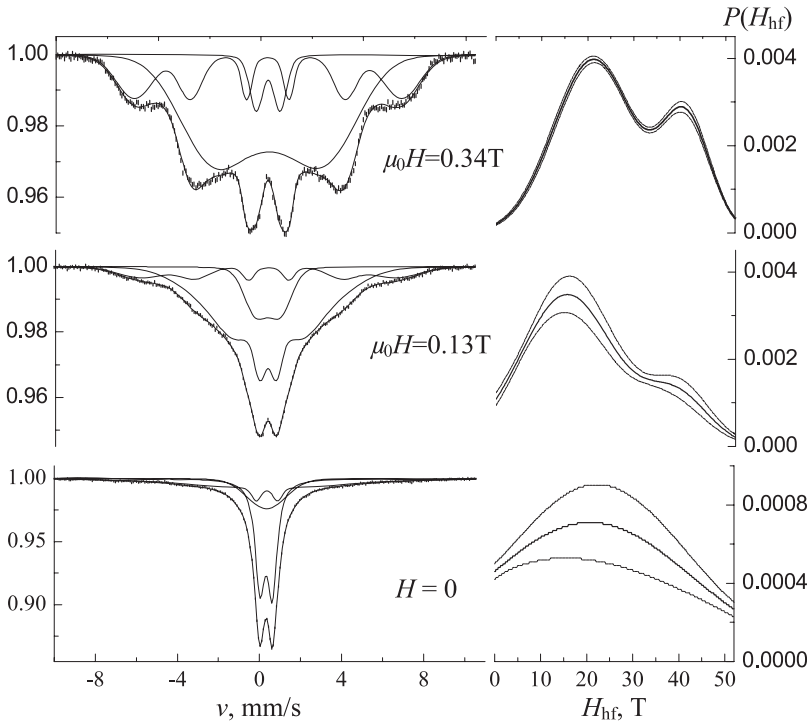

Figure 1. (Left panel) ^{57}Fe Mössbauer spectra (vertical dashes) of iron-oxide nanoparticles (mean size of about 4 nm [38]) in a magnetic field H. Here and below the field direction is perpendicular to the gamma-beam. The resulting and partial spectra (solid lines) are calculated within the corresponding Gaussian hyperfine field distribution $P(H_{\rm hf})$ shown on the right panel and an effective doublet of Gaussian-broadened lines [40].

Such a strange situation with almost diminishing usage of a highly informative and very simple technique, i.e. measurements of the Mössbauer spectra of magnetic nanomaterials in weak static magnetic fields, can be explained by only the fact that there is no theoretical basis which could be used to interpret the field-dependent shape of the spectra at least in the first approximation. The general theory of stochastic relaxation of the uniform magnetization of ferromagnetic single-domain particles was developed by Brown in the early 1960s [31] on the basis of the well known Landau–Lifshitz–Gilbert equation [32, 33]. However, its application in a practical sense is restricted by only numerical simulations without any real analysis of not only the Mössbauer spectra [3, 6], but even magnetization curves [34, 35]. Instead, researchers prefer to interpret the experimental data taken on real samples within the simplest classical models [36, 37], which often reduce to estimates of one or a finite number of empirical parameters such as the blocking temperature, the coercivity, the mean particle size and the magnetic anisotropy constants [9–16, 18–26].

The main goal of the present paper is just to develop such a theory of magnetic dynamics and the corresponding hyperfine interaction, which can be used in numerically analyzing the Mössbauer spectra taken on an ensemble of nanoparticles in a weak static magnetic field. This theory is principally based on the general equations of stochastic relaxation [31], but is reduced to a three-level relaxation model which continues the line of 'physically oriented' phenomenological models of the classical two-level relaxation in the absence of a field [5] and the generalized Stoner–Wohlfarth relaxation in a field [1–4].

2. Hyperfine field distribution

Figure 1 shows the typical ^{57}Fe Mössbauer absorption spectra of nanoparticles of iron oxide in a polymer matrix [38], which were measured in weak magnetic fields (details of the preparation of the samples and Mössbauer measurements can be found in [38]). Because of the absence of a theory to describe or even to qualitatively interpret these spectra at the present time, one can only consider a 'universal' theoretical model used to analyze the Mössbauer spectra of an arbitrary magnetic hyperfine structure and their temperature evolution. This approach is based on the introduction of continuous distributions of the hyperfine field $\boldsymbol{H}_{\rm hf}$ on a nucleus [39]. In this model the absorption spectrum for gamma quanta with energy $E_\gamma = \hbar\omega$ in the presence of the continuous $\boldsymbol{H}_{\rm hf}$ distribution given by the probability function $P(H_{\rm hf})$ is described by the simple expression

$$\bar{\sigma}(\omega) = \int \bar{L}(\omega, H_{\rm hf})\, P(H_{\rm hf})\, {\rm d}H_{\rm hf}, \tag{1}$$

where ω is the spectral frequency,

$$\bar{L}(\omega, H_{\rm hf}) = \frac{\sigma_{\rm a}\Gamma_0^2}{4} \sum_i \frac{A_i}{(\omega - \omega_i(H_{\rm hf}))^2 + \Gamma_0^2/4}, \tag{2}$$

$\sigma_{\rm a}$ is the effective absorber thickness, Γ_0 is the width of the excited nuclear level, A_i is the intensity of the ith hyperfine transition at the resonance frequency

$$\hbar\omega_i(H_{\rm hf}) = E_0 + (m_{\rm e}g_{\rm e} - m_{\rm g}g_{\rm g})\mu_{\rm N}H_{\rm hf}, \tag{3}$$

E_0 is the energy of the resonance transition, μ_N is the nuclear magneton, m_g and m_e are the nuclear spin projections onto the hyperfine field direction, and g_g and g_e are the nuclear g factors for the ground (g) and excited (e) nuclear states, respectively. (For the ^{57}Fe isotope we will refer to below, the nuclear spins $I_g = 1/2$, $I_e = 3/2$ and the M1-type magnetic dipolar radiation occurs, for which transitions with changes in nuclear spin projections of more than unity ($m_g = \pm 1/2 \rightarrow m_e = \mp 3/2$) are forbidden. Hence, the ^{57}Fe partial spectrum (2) consists of not eight lines but six lines, the so-called magnetic sextet.)

The basic advantage of this approach is the simplicity of its computer realization, because it does not require a priori information on the form of the desired distributions. The application of this method allows one formally to reconstruct the $P(H_{hf})$ function for nanoparticles and its temperature evolution from the experimental Mössbauer spectra, which results in qualitative estimates of the abovementioned physical parameters. However, the conventional approach does not provide really quantitative estimates of either the distribution found or the corresponding parameters. The improved variant of this technique allows one to evaluate the resulting hyperfine field distributions with an indication of their mean-square deviations [40]. In this approach additional Gaussian broadening of lines of a magnetic sextet is introduced, which can be regarded as a good estimate for the distribution of the hyperfine field over different sites in the sample, which are represented by the sextet. The resulting H_{hf} distribution can be expressed as a sum over all sextets of Gaussian broadened lines [40]:

$$P(H_{hf}) = \sum_i \frac{A'_i}{\sqrt{2\pi}\gamma_i} \exp\left[-\frac{\left(H_{hf} - \bar{H}^{(i)}_{hf}\right)^2}{2\gamma_i^2}\right] \quad (4)$$

where A'_i is the area of the ith sextet, γ_i is the additional Gaussian linewidth for outer lines of the sextet, and $\bar{H}^{(i)}_{hf}$ is the normalized separation between the outer lines of the sextet. The corresponding distributions evaluated from the Mössbauer spectra shown in figure 1 are displayed in the right-hand panel of the figure. Because the hyperfine field distribution is determined in equation (2) by the parameters of lines, which are adjustable in fitting, one can also estimate the mean-square deviations of $P(H_{hf})$ for each point H_{hf} [40], which are also shown in the right-hand panel of figure 1 by dashed lines.

Even not going into other details, one understands that, in spite of a rather good fit with the experimental spectra, this approach describes only an effective magnetization of the studied ensemble of nanoparticles in a magnetic field, which is, of course, formal in character. In this situation, one should develop a theory for describing the magnetic dynamics in the samples studied and corresponding Mössbauer spectra in order to extract something more real from the experimental spectra.

3. General theory of stochastic relaxation of particle's magnetization

Recently we have developed a unified phenomenological model of magnetic dynamics of an ensemble of single-domain particles, which can be utilized for analyzing both the magnetization curves and the Mössbauer spectra depending on temperature and a magnetic field [1–4]. As a first approximation, we have performed a generalization of the well known Stoner–Wohlfarth model [36] for homogeneously magnetized particles or clusters with uniform magnetization M_0 and uniaxial magnetic anisotropy with energy density K for a more accurate description of relaxation processes within Néel's ideas [37]. The generalized model has been constructed using only the energy density E of such particles in an external magnetic field $\boldsymbol{H}$ [36],

$$E = -K\cos^2\theta - \boldsymbol{H}\boldsymbol{M} \quad (5)$$

(θ is the angle between the easiest magnetization axis and the magnetization vector) and two relaxation parameters making sense of the probabilities of the transitions between two local states with the energy minima $E_i^{(min)}(H, \Theta)$ [2, 4]:

$$p_{12,21}(H, \Theta, T) = \frac{p_0}{2} \times \sum_{i=1,2} \exp\left[-\frac{\left(E_i^{(max)}(H, \Theta) - E_{1,2}^{(min)}(H, \Theta)\right) V}{k_B T}\right] \quad (6)$$

($E_i^{(max)}(H, \Theta)$ are the local energy maxima, Θ is the angle between the external field and the easiest magnetization axis, p_0 is a relaxation parameter slightly depending on temperature T, and V is the particle's volume). A number of magnetization phenomena observed experimentally versus temperature, time, and external magnetic fields can be qualitatively described within this two-level model [2, 4].

The obvious disadvantage of the generalized Stoner–Wohlfarth model is that thermal fluctuations in the local energy minima are not taken into account. In particular, the precession of magnetic moments of nanoparticles in the magnetic anisotropy field and zero external field results in a qualitative transformation of the absorption spectra in the hyperfine field rotating about a certain axis [41, 42]. Even in the simplest case, when the characteristic precession frequency of the particle's magnetization is much higher than the precession frequency of the nuclear spin in the hyperfine field, the effect of fast rotation reduces only to the effective decrease in the hyperfine field [3, 6, 7, 43]:

$$\boldsymbol{H}_{hf}(\theta) = H_{hf}(0)\cos\theta\boldsymbol{n}_z \quad (7)$$

where $\boldsymbol{n}_z$ is the unit vector along the anisotropy axis. It is clear that the effects of the precession of the particle's magnetization in an external magnetic field should be more complicated and must be taken into account. Let us try to do so.

The general theory of the stochastic relaxation of the uniform magnetization $\boldsymbol{M}$ for the statistical ensemble of ferromagnetic single-domain particles is based on the following 'Langevin equation' describing the reorientation of the vector $\boldsymbol{M}$ in the presence of a rapidly fluctuating chaotic field $\boldsymbol{h}(t)$ [31]:

$$\frac{d\boldsymbol{M}}{dt} = \gamma\boldsymbol{M} \times \left[\boldsymbol{H}_{eff} - \eta\frac{d\boldsymbol{M}}{dt} + \boldsymbol{h}(t)\right] \quad (8)$$

where γ is the gyromagnetic ratio, η is the dissipation coefficient,

$$\boldsymbol{H}_{\text{eff}} \equiv \boldsymbol{H}_{\text{eff}}(\theta, \varphi) = -\frac{V}{M_0}\nabla E(\theta, \varphi) \tag{9}$$

where θ and φ are the polar and azimuth angles, respectively, defining the direction of the vector $\boldsymbol{M}$. Under the assumption that the stochastic process $\boldsymbol{h}(t)$ is stationary and isotropic, i.e.

$$\langle h_i(t)\rangle = 0, \qquad \left\langle h_i(t)h_j(t+\tau)\right\rangle = \mu\delta_{ij}\delta(\tau). \tag{10}$$

Brown has derived the following differential equation for the probability density (population) $W(\theta, \varphi)$ of states with a given direction of the vector $\boldsymbol{M}$:

$$\frac{\partial W}{\partial t} = -\hat{P}W \tag{11}$$

where

$$\hat{P} = -D\left[\Delta - \frac{V}{kT}\nabla\left(\nabla E(\theta, \varphi)\right)\right] - \frac{\gamma}{M_0}\nabla\left(\frac{\boldsymbol{M}}{M_0} \times \nabla E(\theta, \varphi)\right) \tag{12}$$

is the diffusion operator in the representation given in [44], and the diffusion coefficient satisfies the Einstein relation

$$D = \frac{\gamma\eta k_{\text{B}}T}{VM_0} = \frac{\gamma\mu}{2M_0}. \tag{13}$$

The relaxation operator given by equation (12) has the form of the Fokker–Planck operator and its terms describe the isotropic diffusion, drift towards the local minima of the anisotropy energy, and precession of the vector $\boldsymbol{M}$ in the effective field $\boldsymbol{H}_{\text{eff}}$ (figure 2), respectively.

Since classical work [31], the analytic properties of differential equation (11) have been studied for the simplest case of the longitudinal relaxation, where the external field is directed along the magnetic anisotropy axis. In this case, potential (5) is axially symmetric, homogeneous precession does not affect the relaxation properties, and the populations of the states, $W(\theta, \varphi)$, are independent of the azimuth angle φ. Correspondingly, the equilibrium state of the particle ensemble is described by the Gibbs distribution over the stochastic states, i.e. over the precession orbits of the end of vector $\boldsymbol{M}$ on the sphere of radius M_0 about the easy axis with a given θ value:

$$W(\theta) \propto \sin\theta \exp\left[-\frac{E(\theta)V}{k_{\text{B}}T}\right]. \tag{14}$$

However, this approach is not applicable to describe the Mössbauer spectra of nanoparticles with the chaotic distribution of the anisotropy axes, when it is necessary to consider the arbitrary orientation of vector $\boldsymbol{H}$ with respect to the magnetic anisotropy axis in equation (5), i.e. to take into account the dependence on angle φ in equations (8)–(12).

On the other side, the relaxation model for describing the Mössbauer spectra of nanoparticles in the absence of an external magnetic field has been defined within the quantum mechanical description of a nanoparticle with the total spin S and $2S + 1$ possible states of the projection S_z, the transitions

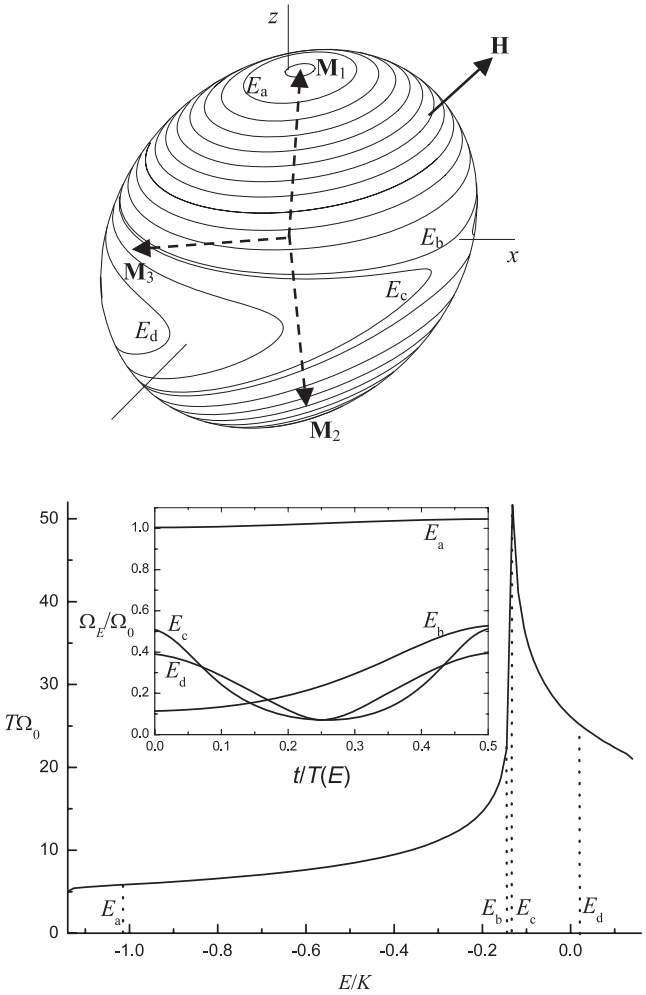

Figure 2. (Top) Constant energy levels (trajectories of the uniform magnetization's precession over the sphere with radius M_0) for single-domain particles with the uniaxial magnetic anisotropy in a magnetic field $\boldsymbol{H}$ ($h = 0.1$, $\Theta = 45°$). Dashed lines show the directions of the magnetization vector corresponding to the local energy minima ($\boldsymbol{M}_1$ and $\boldsymbol{M}_2$) and the absolute maximum ($\boldsymbol{M}_3$) of energy (5). (Bottom) Energy dependence of the period of the uniform magnetization's precession along the corresponding trajectory C_E. The inset shows the time dependence of the angular velocity along the selected trajectories C_E with the given energies E_{a}, E_{b}, E_{c} and E_{d}.

between these states being determined under the assumption that relaxation is associated with the transverse components of the random field $\boldsymbol{h}(t)$ [3, 6]. From the macroscopic viewpoint this one-dimensional model describes stochastic transitions between orbits of the uniform magnetization precession (with constant energy $E(\theta)$) in the effective field

$$\boldsymbol{H}_{\text{eff}}(\theta) = H_{\text{eff}}(0)\cos\theta\boldsymbol{n}_z, \tag{15a}$$

where the parameter

$$H_{\text{eff}}(0) = 2KV/M_0 \tag{15b}$$

defines the characteristic precession frequency

$$\Omega_0 = -\gamma H_{\text{eff}}(0). \tag{15c}$$

This approach can be applied to our case for describing the magnetic dynamics and the relaxation Mössbauer spectra of nanoparticles in a magnetic field, taking into account the most significant points in this changed situation, i.e. the complication of the form of the relaxation matrix specified by equation (12) and the appearance of an inhomogeneous precession in the effective field $\boldsymbol{H}_{\text{eff}}$ given by equation (9). As clearly seen in figure 2, in a magnetic field with strength lower than the critical value $H_C(\theta)$ [2, 36], the vector $\boldsymbol{M}$ for a given energy E in the absence of dissipation describes a conic surface around one of the three poles corresponding to two local minima and the absolute maximum of energy (5). Here and below, the external magnetic field is written in the normalized form [36]:

$$h = HM_0/2K. \tag{16}$$

The shapes of the precession orbits are determined by the Hamiltonian (5) and obvious relation

$$M_x^2 + M_y^2 + M_z^2 = M_0^2, \tag{17}$$

the time dependence of the precession of the vector $\boldsymbol{M}(E, \Theta)$ along each trajectory C_E is defined by equations (8) and (9) in the absence of dissipation, while the corresponding precession period is determined by the elliptic integral along the corresponding trajectory C_E in view of equations (5), (8), and (9),

$$T(E, \Theta) = \frac{1}{\Omega_0 h \sin\Theta} \int_{C_E} \frac{\mathrm{d}m_z}{\sqrt{1 - m_x^2 - m_z^2}} \tag{18}$$

where the normalized projections of the vector $\boldsymbol{M}(E, \Theta)$ are introduced:

$$m_{x,z} \equiv \frac{M_{x,z}(E, \Theta)}{M_0} \tag{19}$$

which are related to each other and to the given energy E by equation (5). The precession period versus energy is shown at the bottom of figure 2, which clearly manifests a strong increase in the period for energy values corresponding the equatorial trajectories on the top of this figure in accordance with zero precession frequency for $\theta = \pi/2$ in zero field (see equation (15)).

However, the most important feature arising in an applied magnetic field is that the angular velocity of precession specified by the effective field (9) changes continuously both in magnitude and in direction along each trajectory C_E:

$$\Omega_E(\theta, \varphi, \Theta) = \Omega_0 \sqrt{m_z^2(\theta, \varphi) + 2hm_z(\theta, \varphi)\cos\Theta + h^2}. \tag{20}$$

(Note that the angular velocity (20) is not equal to zero at each point (θ, φ) of each trajectory C_E, in contrast to the case of axial symmetry for $H = 0$ and/or $\Theta = 0$ [3, 41, 42].) In this case, if the constant D of the isotropic diffusion is not much higher than the characteristic frequency of precession along a given trajectory C_E, the populations of the states, $W_E(\theta, \varphi)$, with the same energy E at different points (θ, φ) of this trajectory are inversely proportional to the effective (corrected by diffusion) instantaneous angular velocity at these points [44]. The time dependence of the angular velocity along the selected trajectories C_E is shown in the inset of figure 2, where the minimum value of the angular velocity Ω_E for a given energy E corresponds to the maximal projection $M_x(E, \Theta)$.

This fact drastically changes the conventional scheme for calculations of both the average magnetization and Mössbauer absorption spectra of an ensemble of single-domain particles. According to a schematic consideration in [44], in this case the very precession orbits C_E can be considered as stochastic states of each particle. Then, in the case of slow diffusion ($D \ll \Omega_0$) each state (orbit) can be characterized by the mean magnetization $\bar{M}(E, \Theta)$, which is again determined by the elliptic integrals along the corresponding trajectory C_E according to equations (8) and (9):

$$\bar{M}_{z,x}(E, \Theta) = \frac{1}{T(E, \Theta)\Omega_0 h \sin\Theta} \int_{C_E} \frac{M_{z,x}\,\mathrm{d}m_z}{\sqrt{1 - m_x^2 - m_z^2}} \tag{21a}$$

and the symmetry condition

$$\bar{M}_y(E, \Theta) = 0. \tag{21b}$$

Furthermore, it is necessary to determine the probability of the transition per unit time between the stochastic states specified by, e.g., the statistical characteristic of the random field $\boldsymbol{h}(t)$ by analogy with [3, 6, 31]. Thus, the model of magnetic dynamics for calculating the magnetic characteristics in various measurement methods, including the Mössbauer spectroscopy, becomes determined.

4. Three-level relaxation model

It is not difficult to write the general expression for the Mössbauer absorption spectrum in the representation given in the previous section; however, the main problems of analysis are associated with the optimization of a calculation procedure, first of all for calculation of the Liouville hyperfine-interaction superoperators [2] under the average magnetization $\bar{M}(E, \Theta)$ changing continuously both in magnitude and in direction and the corresponding average hyperfine field $\bar{\boldsymbol{H}}_{\text{hf}}(E, \Theta) \propto \bar{\boldsymbol{M}}(E, \Theta)$ for different orbits and Θ. This is why we will consider here a simplified version of such a model, which allows one not only to analyze (in the first approximation) the experimental Mössbauer spectra of an ensemble of nanoparticles in a magnetic field, but also to make qualitative conclusions on specific shapes of the absorption spectra in this case.

At first glance, this task can be reduced to a formal specification of the generalized Stoner–Wohlfarth model [2, 4] based on equations (5) and (6) to the case of three-dimensional character of the energy barrier between the local energy minima. That is, one can average the uniform magnetization over thermal fluctuations into each local energy minimum by analogy with the well known approximation [43]

$$\bar{M}_i(T, \Theta) = \int_{E_i^{(\min)}(H,\Theta)}^{E_1^{(\max)}(H,\Theta)} \bar{M}(E, \Theta) W_i(E, T, \Theta)\,\mathrm{d}E \tag{22a}$$

where

$$W_i(E, T, \Theta) = \frac{1}{Z_i} \exp(-EV/kT) \int_{C_E} \mathrm{d}\Omega. \tag{22b}$$

The integral in equation (22*b*) is taken over the solid angle along the corresponding trajectory C_E and the normalization constants Z_i are defined by the condition

$$\int_{E_i^{(\min)}(H,\Theta)}^{E_1^{(\max)}(H,\Theta)} W_i(E, T, \Theta)\, \mathrm{d}E = 1. \tag{22c}$$

However, as clearly seen in figure 2, the region of stable rotation about the pole corresponding to the absolute energy maximum $E_2^{(\max)}$ takes a substantial fraction of the stochastic space (points over the unit sphere), that is increasing with the strength of an external magnetic field. When $H > H_C(\theta)$, there remains a single energy minimum characterized by the mean magnetization $\bar{M}_1(T, \Theta)$. This is why this region must be taken into account in developing the relaxation model for the description of both the magnetic dynamics and corresponding Mössbauer spectra of an ensemble of single-domain particles. Thus, we come to the three-level relaxation model within the stochastic states characterized by the mean magnetizations $\bar{M}_i(T, \Theta)$ ($\bar{M}_3(T, \Theta)$ defined by equation (22*a*), where the integration limits are $E_1^{(\max)}$ and $E_2^{(\max)}$) and the equilibrium populations determined by the obvious relation

$$\bar{W}_i = Z_i/(Z_1 + Z_2 + Z_3). \tag{23}$$

Now one has to define a relaxation model, i.e. the probabilities of transitions per unit time between the three stochastic states. Assuming that the relaxation between the states occurs as a random walk of the vector $\boldsymbol{M}$ with small step lengths (rotation by a small angle), the transitions between the states corresponding to local energy minima occur only through state 3 corresponding to the absolute energy maximum (see figure 2), i.e., $p_{12} = p_{21} = 0$ [6]. Then, the other relaxation rates are determined by the detailed balance principle:

$$p_{3i} = p_0, \tag{24a}$$

$$p_{i3} = p_{3i} \frac{\bar{W}_3}{\bar{W}_i}. \tag{24b}$$

Here, $i = 1, 2$ and p_0 is a phenomenological constant specified by, e.g., the statistical characteristics of the random field $\boldsymbol{h}(t)$ by analogy with [3, 6, 31]. Thus, the three-level relaxation model is completely defined.

5. Mössbauer spectra within the three-level relaxation model

The calculation of Mössbauer spectra within the three-level relaxation model defined by equations (21)–(24) can be performed in terms of the Anderson's stochastic approach [45], according to which the absorption spectrum is described by the general expression [2, 46, 47]

$$\sigma(\omega, \Theta) = -\frac{\sigma_a \Gamma_0}{2} \mathrm{Im} \sum_\eta \mathrm{Sp}\left(\hat{V}_\eta \langle W| \hat{\mathbf{A}}^{-1}(\omega, \Theta) |1\rangle \hat{V}_\eta^+\right) \tag{25}$$

where $\hat{V}_\eta$ is the operator for the interaction of the gamma-quantum with a given polarization η and the nucleus, $\langle W|$ is the row vector of the occupation probabilities of the stochastic states in equilibrium, $|1\rangle$ is a column vector with all components equal to unity and the superoperator

$$\hat{\mathbf{A}}(\omega, \Theta) = \omega - \hat{\mathbf{L}}_{\mathrm{hf}}(\Theta) + \mathrm{i}\hat{\mathbf{P}}(\Theta) + \mathrm{i}\Gamma_0/2 \tag{26}$$

is defined by the Liouville operator of hyperfine interaction that is diagonal over the stochastic states,

$$\langle \mathrm{i}| \hat{\mathbf{L}}_{\mathrm{hf}}(\Theta) |j\rangle = \hat{\mathbf{L}}_{\hat{H}}(\bar{M}_i(\Theta))\delta_{ij} \tag{27}$$

and the relaxation matrix

$$\hat{\mathbf{P}} = \hat{P} \otimes \hat{\mathbf{1}}_{\mathrm{n}}, \tag{28a}$$

$$P_{ij} = \underset{j \neq i}{} p_{ij}, \tag{28b}$$

$$P_{ii} = -\sum_{j \neq i} p_{ij}. \tag{28c}$$

Here, the superoperator $\hat{\mathbf{L}}_{\hat{H}}(\bar{M}_i(\Theta))$ acts in the space of $(2I_g + 1)(2I_e + 1)$ nuclear variables [48],

$$(\hat{\mathbf{L}}_{\hat{H}})_{m_e m_g m'_e m'_g} = H^{(e)}_{m_e m'_e} \delta_{m_g m'_g} - H^{(g)}_{m_g m'_g} \delta_{m_e m'_e}, \tag{29}$$

i.e. is determined by the Hamiltonians of hyperfine interaction for the ground and excited states, which in our case take the forms

$$\hat{H}_i^{(g,e)}(\Theta) = -g_{g,e}\mu_N H_{\mathrm{hf}}^{(0)} \frac{\hat{\boldsymbol{I}}^{(g,e)} \bar{M}_i(\Theta)}{M_0} \tag{30}$$

where $H_{\mathrm{hf}}^{(0)}$ is the hyperfine field at extremely low temperature, $\hat{\boldsymbol{I}}^{(g,e)}$ is the operator of nuclear spin, and $\hat{\mathbf{1}}_n$ is the identity superoperator in the space of nuclear variables.

The resulting absorption spectrum of an ensemble of single-domain particles is defined by the sum over polarization η according to the scheme proposed in [47] and the averaging of partial spectra (25) over the chaotic distribution of the anisotropy axes:

$$\sigma(\omega) = \int \sigma(\omega, \Theta) \sin\Theta \, \mathrm{d}\Theta. \tag{31}$$

Using equations (25)–(31) one can calculate the Mössbauer absorption spectrum in the framework of the three-level relaxation model (21)–(24) for given values of external (H and T) and intrinsic ($H_{\mathrm{hf}}^{(0)}$, K, V, M_0, and p_0) parameters.

Figure 3 shows typical ^{57}Fe Mössbauer absorption spectra calculated within the three-level relaxation model for various values of the normalized external field h and the effective energy barrier KV/k_BT. (Note that the rank of matrices (26) in this case is equal to 24.) Along with the obvious effect of the resulting magnetization of the ensemble of nanoparticles in a field, a great diversity of the spectral shapes observed in the figure reflects a non-trivial character of the local and equilibrium magnetization at different values of temperature and field. The spectra in the negligible field ($h = 0.01$) display a slightly resolved magnetic hyperfine structure (sextet of lines) and a collapsed (due to relaxation) central line. In

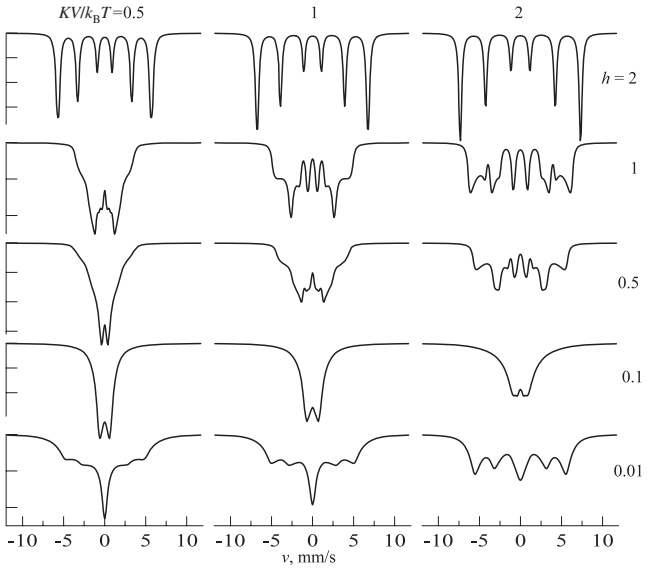

Figure 3. ^{57}Fe Mössbauer spectra of an ensemble of nanoparticles ($\mu_0 H_{\rm hf}^{(0)} = 50$ T, $p_0 = 1$ GHz) in a magnetic field, calculated in the three-level relaxation model as a function of the effective energy barrier KV/k_BT (from left to right) and the normalized field strength h (from top to bottom).

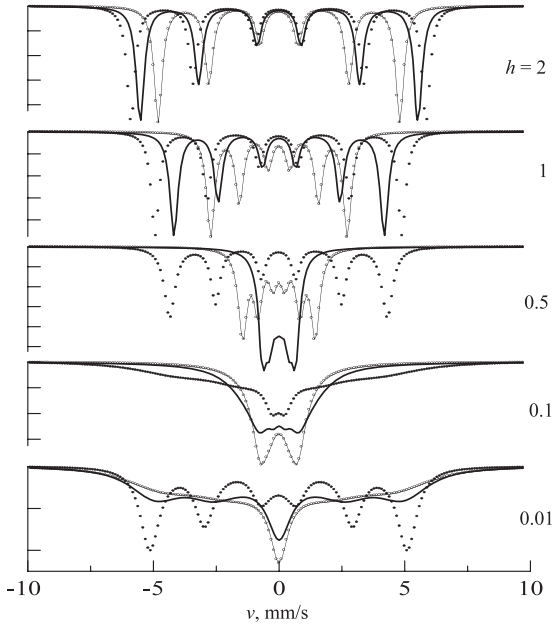

Figure 4. Partial absorption spectra of particles ($\mu_0 H_{\rm hf}^{(0)} = 50$ T, $p_0 = 1$ GHz, $KV/k_BT = 1$) as calculated in the three-level relaxation model for different orientations of the anisotropy axis with $\Theta = 10°$ (points), 45° (solid lines), and 80° (open circles) in a magnetic field of different strengths h (from top to bottom).

a stronger, but still weak, field ($h = 0.1$), the magnetic hyperfine structure visually disappears and the spectra look like a doublet of lines with the splitting slightly depending on the effective energy barrier, i.e. on temperature and/or the particle size. The spectra of the magnetic nanomaterials often certainly exhibit line doublets [3, 19–28] (see also figure 1), which are usually attributed to the presence of the quadrupole hyperfine interaction in the presence of the electric field gradient on the nucleus. However, such interpretation often seems very artificial; for example, such a 'doublet' is often realized at higher temperatures, but quadrupole splitting is completely absent in the spectra at lower temperatures. Such behavior suggests that the observed 'doublets' are likely of magnetic rather than electric nature [3], which is also justified by the present calculations, where the quadrupole hyperfine interaction is not taken into account.

With external field increasing ($h = 0.5$ and 1) there again appears a resolved magnetic hyperfine structure on the background of the 'doublet' in the spectra. In a strong magnetic field ($h = 2$) the magnetic hyperfine structure becomes well resolved. Indeed, such a transformation of the spectral shape with field changing is directly related to the longstanding and heated debates of two research groups on pages of authoritative journals (see [49–52] and references therein). One of the groups contended that the presence of interparticle interaction, i.e. a mean ('molecular') field at each particle in the ensemble, results in fastening the magnetization's relaxation, whereas the other made the contrary assertion, i.e., 'an applied field' is slowing down the relaxation. Not going into details, note that all the arguments of both the groups were based on the estimates of average relaxation time (the probabilities of transitions) between two local energy minima. However, the latter are obviously nonequivalent in a magnetic field and the probabilities of transitions from one state to the other are different, which defines local relaxation magnetic properties as a consequence of the asymmetric magnetization fluctuations resulting in specific shapes of Mössbauer spectra [21, 53]. Nevertheless, the spectra shown in figure 3 manifest both the speeding up ($h = 0.1$) and slowing down ($h \geqslant 0.5$) relaxation in a magnetic field (or in the presence of the mean-field interaction), which actually justifies both conclusions of the two groups.

A qualitative character of such a behavior of the local magnetization can be clarified if one considers the limiting case of weak magnetic field ($h \ll 1$) when [17]

$$E_{1,2}^{(\min)}(H, \Theta) \approx -KV\,(1 \pm 2h\cos\Theta) \qquad (32a)$$

and

$$E_{1,2}^{(\max)}(H, \Theta) \approx \pm 2hKV\sin\Theta \qquad (32b)$$

up to the terms linear in h. As clearly seen from these equations, barrier for local (not absolute) energy minimum 2 is always decreasing with h increasing, which evidences for the fastening the relaxation of this local state. Another situation occurs for the absolute energy minimum 1, when the local energy barrier is decreasing with h increasing only for the particles with $\Theta \geqslant \pi/4$, while the barrier for the particles with smaller Θ is increasing with h. This is why both the effective fastening and slowing down relaxation are observed in the Mössbauer spectra of nanoparticles [21, 49–52]. This effect is demonstrated in figure 4 where the partial Mössbauer spectra of particles with different orientation of the anisotropy axis are shown. This figure also helps one to understand the specific shapes of the resulting absorption spectra of an ensemble of particles, which are shown in figure 3.

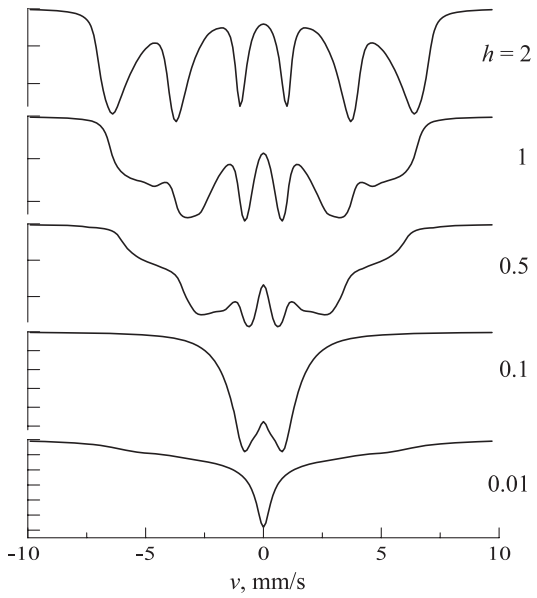

Figure 5. ^{57}Fe Mössbauer spectra of an ensemble of nanoparticles ($\mu_0 H_{\rm hf}^{(0)} = 50$ T, $p_0 = 3$ GHz) as calculated in the three-level relaxation model for the Gaussian distribution of the particle volume ($K\bar{V}/k_{\rm B}T = 1$ and $\sigma_V/\bar{V} = 0.5$) in a magnetic field of different strengths h (from top to bottom).

The comparison of the Mössbauer spectra calculated within the three-level model (figures 3 and 4) with the experimental data (see figure 1) shows that the lineshapes are much wider in the experimental curves owing to the natural distribution of the physical parameters in the sample under investigation, e.g. the volume distribution of particles $P(V)$. In this case, the resulting Mössbauer spectra of the ensemble of particles are expressed as

$$\bar{\sigma}(\omega) = \frac{1}{Z_V}\int \sigma(\omega) V P(V)\,{\rm d}V \qquad (33a)$$

where Z_V is the normalization constant:

$$Z_V = \int V P(V)\,{\rm d}V. \qquad (33b)$$

Figure 5 shows typical ^{57}Fe Mössbauer absorption spectra of the ensemble of nanoparticles calculated within the three-level relaxation model for various values of the normalized external field h and the Gaussian distribution of particle volume:

$$P(V > 0) = \exp\left(-\frac{(V-\bar{V})^2}{2\sigma_V^2}\right). \qquad (34)$$

The transformation of the spectra with increasing field qualitatively reproduces the evolution of the experimental spectra shown in figure 1. Moreover, an effective 'doublet' of lines in a weak magnetic field ($h = 0.1$) is clearly observed in the volume-averaged spectra due to slight dependence of its splitting on the effective energy barrier (particle size and/or temperature) as seen in figure 3.

The formalism described above principally allows one to fit the experimental Mössbauer absorption spectra like those shown in figure 1 and to determine the parameters ($H_{\rm hf}^{(0)}$, K, $\bar{V}$, σ_V, M_0 and p_0) inherent to the sample under investigation. However, this problem requires a separate, primarily qualitative analysis in order to optimize the corresponding calculation procedure and results will be published elsewhere. Let us consider here one more qualitative point, namely, the Mössbauer lineshape for an ensemble of nanoparticles in the limiting case of high temperature.

6. High-temperature limit

First, we come back to the limiting case of a weak magnetic field ($h \ll 1$) when the population of level 3 can be neglected. In the high-temperature limit ($k_{\rm B}T \gg KV$), when the regime of fast relaxation between states 1 and 2 of local energy minima is realized, the hyperfine field $H_{\rm hf}$ over the nuclear lifetime is proportional to the mean magnetization of each particle with a given Θ:

$$\bar{M}(\Theta) = \bar{W}_1(\Theta)\bar{M}_1(\Theta) + \bar{W}_2(\Theta)\bar{M}_2(\Theta). \qquad (35)$$

Then, the absorption spectrum (25) in the fast relaxation regime is defined by the mean Liouville operator of hyperfine interaction averaged over the stochastic states [2]:

$$\bar{\hat{\mathbf{L}}}_{\rm hf}(\Theta) = \bar{W}_1(\Theta)\hat{\mathbf{L}}_H(\bar{M}_1(\Theta)) + \bar{W}_2(\Theta)\hat{\mathbf{L}}_H(\bar{M}_2(\Theta)) = \hat{\mathbf{L}}_H(\bar{M}(\Theta)). \qquad (36)$$

In this case the Mössbauer absorption spectrum of an ensemble of particles is determined by equations (1)–(3), where

$$P(H_{\rm hf}) = \frac{M_0}{H_{\rm hf}^{(0)}\left(\partial\bar{M}(\Theta)/\partial\cos\Theta\right)}. \qquad (37)$$

A routine analysis of equations (22) and (23) in this limiting case allows one to estimate the lower boundary for the mean magnetization as follows:

$$\bar{M}(\Theta) \approx M_0\sqrt{\frac{h^2}{4}\sin^2\Theta + \frac{x^2}{9}\cos^2\Theta}, \qquad (38)$$

where

$$x = M_0 H V/k_{\rm B}T,$$

is the parameter of the Langevin function [54]. Equation (38) defines the asymptotic trend of the local magnetization for each group of particles with the given Θ to a constant with temperature increasing in complete analogy with the asymptotic behavior of magnetization and susceptibility in the high-temperature limit [17], which is different from the Langevin limit for ideal superparamagnetic particles [55].

Taking into account equations (35)–(38), the Mössbauer absorption spectrum of an ensemble of particles is defined by equations (1)–(3) with the hyperfine field distribution

$$P(H_{\rm hf}) = \frac{1}{H_{\rm hf}^{(0)}\sqrt{h^2/4 - x^2/9}}\frac{h_{\rm hf}}{\sqrt{h^2/4 - h_{\rm hf}^2}} \qquad (39a)$$

where non-zero values of $P(H_{\rm hf})$ are realized in the interval

$$x/3 < h_{\rm hf} = \frac{H_{\rm hf}}{H_{\rm hf}^{(0)}} < h/2. \qquad (39b)$$

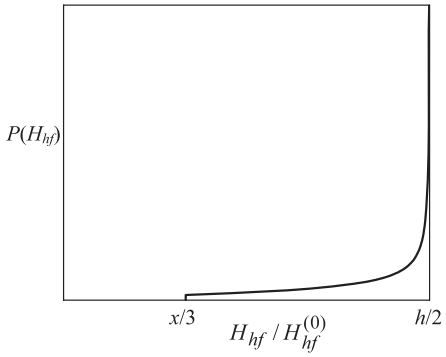

Figure 6. Hyperfine field distribution $P(H_{\rm hf})$ within the three-level relaxation model and the limiting case of a weak magnetic field ($h \ll 1$) and high temperature ($k_{\rm B}T \gg KV$).

The probability function (39) is shown in figure 6, that demonstrates that the effective distribution $P(H_{\rm hf})$ for $h \ll 1$ appears to be rather narrow and concentrated at the upper boundary of the interval (39*b*). That is, the distribution actually describes the effective 'doublets' of lines in figures 3–5 and points to a magnetic nature of the doublet observed in figure 1 at $H = 0$, which can be explained, for instance, by the presence of a weak interaction between particles in the sample studied.

In stronger fields the hyperfine field distribution $P(H_{\rm hf})$ broadens: the contribution of the effective magnetic 'doublet' to the absorption intensity decreases and there appears a slightly resolved hyperfine structure on the background of the doublet (figures 3–5). In the strong magnetic field limit ($h \gg 1$) a single local energy minimum is realized, so one can estimate from equation (22) the mean magnetization of each particle at high temperature ($k_{\rm B}T \gg HM_0V$):

$$\bar{M}(\Theta) \approx M_0 \left(\frac{x}{3} + \frac{\pi}{16} \frac{KV}{k_{\rm B}T} \sin 2\Theta \right). \qquad (40)$$

Here, the first term in the brackets in equation (40) is the classical high-temperature limit of the Langevin function for ideal superparamagnetic particles, whereas the second term is a correction for the magnetic anisotropy. The absorption spectrum of an ensemble of particles in this case is again defined by equations (1)–(3), where the effective distribution $P(H_{\rm hf})$ is concentrated in the vicinity of $H_{\rm hf} = H_{\rm hf}^{(0)} x/3$ and defines the shape of spectra shown in figures 1 and 3 ($h = 2$).

7. Conclusions

Thus, the three-level relaxation model presented above and taking into account the magnetic anisotropy, precession and diffusion of uniform magnetization can be efficiently used to describe the experimental Mössbauer absorption spectra of an ensemble of magnetic nanoparticles in a weak magnetic field. This model allows one to take into consideration physical mechanisms of formation of the magnetic hyperfine structure within the magnetic dynamics inherent to such materials. A number of qualitative effects observed in experimental Mössbauer spectra taken on small magnetic particles even in zero magnetic field can be self-consistently explained within the model in terms of the mean-field interparticle interaction. In particular, this model predicts the appearance of ^{57}Fe magnetic sextets with a small hyperfine splitting slightly dependent on the particle size and temperature in a weak magnetic field and at high temperature, which look like effective 'doublets' of lines often observed in experimental spectra. Such magnetic 'doublets' should be taken into account in treating the experimental Mössbauer spectra along with conventional doublets of lines arising from the quadrupole hyperfine interaction of electric nature.

This relaxation model can be also efficiently used for analyzing the magnetization curves [8–17] as well as being modified to describe the interacting single-domain particles in the framework of the mean-field approximation [1, 21, 49–53], which will significantly expand its application area for analyzing experimental data. At the same time, it should be taken into account that this model is adequate in the slow diffusion limit when the isotropic diffusion constant is much less than the characteristic frequency of the uniform magnetization's precession, so more accurate models for analyzing both the Mössbauer absorption spectra and magnetization curves should be developed, which help one to get more specific information about the samples studied as compared to the results of the analysis presented here.

In order to describe the magnetic dynamics of an ensemble of single-domain particles in the general case one should consider a multi-level model taking into account a continuous relaxation process with the inclusion of the diffusion and precession of uniform magnetization. Retaining the main idea of the general approach presented in section 3, where the precession orbits with a given energy value are regarded as stochastic states of each particle, the probabilities of transitions per unit time between the stochastic states (orbits) can be determined by the components of the random field (10) which are transverse to the instantaneous value of the effective field (9) at each point (θ, φ) of the adjacent orbits, by analogy with the microscopic model developed in the absence of an external magnetic field [3, 6]. In fact, such a model for describing the equilibrium magnetization of an ensemble of particles has been already developed and the results will be published soon [56]. In particular, the non-Langevin asymptotic behavior of high-temperature magnetization, which is predicted within the two-level model [17] and revealed specifically in the Mössbauer spectra according to equation (38), remains qualitatively within the multi-level model and is even experimentally observed [56].

The Mössbauer spectra of an ensemble of single-domain particles in a magnetic field can be also described within the multi-level model using the same equations (25)–(31) with the superoperators of a more general form defined by matrices of a higher rank $N = (2S + 1)(2I_{\rm g} + 1)(2I_{\rm e} + 1)$ where S is the total particle spin (see, e.g., [3, 6]). Therefore, the main problems of analysis are associated with the optimization of a calculation procedure dealing with the Liouville operators staying in equation (26) under the average magnetization $\bar{M}(E, \Theta)$ changing continuously both in magnitude and in direction and the corresponding average hyperfine field $\bar{H}_{\rm hf}(E, \Theta) \propto \bar{M}(E, \Theta)$. At first glance, this task seems

to be extremely cumbersome because, first of all, S is about 1000 for real nanoparticles. However, the relaxation matrix $\hat{P}$ in the multi-level model is actually a superposition of tridiagonal terms due to a thermal activation between the adjacent trajectories [3, 6] and two additional (non-tridiagonal) elements that describe the rates of relaxation transitions between the energy level first excited as compared to the local energy maximum $E_1^{(\max)}$ and the most excited energy level in the local minimum 2 (see, e.g., orbits labeled E_c and E_b in figure 2). This form of the relaxation matrix allows one to reduce the superoperator $\hat{A}(\omega, \Theta)$ specified by equation (26) to a tridiagonal block form in the space of the stochastic states by means of an orthogonal transformation, which, in turn, essentially simplifies calculations by equation (25). Studies in this direction are in progress.

Acknowledgments

I am sincerely grateful to Dr V M Cherepanov for the experimental spectra and the Russian Foundation for Basic Research (project No 08-02-00388) for the financial support.

References

[1] Afanas'ev A M, Chuev M A and Hesse J 1997 *Phys. Rev.* B **56** 5489
[2] Afanas'ev A M, Chuev M A and Hesse J 1999 *JETP* **89** 533
[3] Chuev M A 2006 *JETP Lett.* **83** 572
[4] Chuev M A and Hesse J 2007 *J. Phys.: Condens. Matter* **19** 506201
[5] Wickman H H 1966 *Mössbauer Effect Methodology* vol 2, ed I J Gruverman (New York: Plenum)
[6] Jones D H and Srivastava K K P 1986 *Phys. Rev.* B **34** 7542
[7] van Lierop J and Ryan D H 2001 *Phys. Rev.* B **63** 064406
[8] Hesse J, Bremers H, Hupe O, Veith M, Fritscher E W and Valtchev K 2000 *J. Magn. Magn. Mater.* **212** 153
[9] Jönsson P, Hansen M F and Nordblad P 2000 *Phys. Rev.* B **61** 1261
[10] Wernsdorfer W, Thirion C, Demoncy N, Pascard H and Mailly D 2002 *J. Magn. Magn. Mater.* **242–245** 132
[11] Rellinghaus B, Stappert S, Acet M and Wassermann E F 2003 *J. Magn. Magn. Mater.* **266** 142
[12] Michele O, Hesse J, Bremers H, Polychroniadis E K, Efthimiadis K G and Ahlers H 2004 *J. Phys.: Condens. Matter* **16** 427
[13] Michele O, Hesse J, Bremers H, Wojczykowski K, Jutzi P, Sudfeld D, Ennen I, Hütten A and Reiss G 2004 *Phys. Status Solidi* C1 **12** 3596
[14] Cador O, Grasset F, Haneda H and Etournea J 2004 *J. Magn. Magn. Mater.* **268** 232
[15] Michele O, Hesse J and Bremers H 2006 *J. Phys.: Condens. Matter* **18** 4921
[16] Du J, Zhang B, Zheng R K and Zhang X X 2007 *Phys. Rev.* B **75** 014415
[17] Chuev M A 2007 *JETP Lett.* **85** 611
[18] Suzuki K and Cadogan J M 1998 *Phys. Rev.* B **58** 2730
[19] Hupe O, Chuev M A, Bremers H, Hesse J and Afanas'ev A M 1999 *Nanostruct. Mater.* **12** 581
Hupe O, Chuev M A, Bremers H, Hesse J and Afanas'ev A M 1999 *J. Phys.: Condens. Matter* **11** 10545
[20] Balogh J, Bujdoso L, Kaptás D, Keméni T, Vincze I, Szabó S and Beke D L 2000 *Phys. Rev.* B **61** 4109
[21] Chuev M A, Hupe O, Afanas'ev A M, Bremers H and Hesse J 2002 *JETP Lett.* **76** 558
[22] Predoi D, Kuncser V, Tronc E, Nogues M, Russo U, Principi G and Filoti G 2003 *J. Phys.: Condens. Matter* **15** 1797
[23] Stankov S, Sepiol B, Kanuch T, Scherjau D, Würschum R and Miglierini M 2005 *J. Phys.: Condens. Matter* **17** 3183
[24] Hendriksen P V, Bødker F, Linderoth S, Wells S and Mørup S 1994 *J. Phys.: Condens. Matter* **6** 3081
[25] Vasquez-Mansilla M, Zysler R D, Arciprete C, Dimitrijewits M I, Saragovi C and Greneche J M 1999 *J. Magn. Magn. Mater.* **204** 29
[26] Tronc E, Ezzir A, Cherkaoui R, Chanéac C, Nougés M, Kachkachi H, Fiorani D, Testa A M, Grenèche J M and Joulivet J P 2000 *J. Magn. Magn. Mater* **37** 39
[27] Eibschüts M and Shtrikman S 1968 *J. Appl. Phys.* **39** 997
[28] Lindquist R H, Constabaris G, Kündig W and Portis A M 1968 *J. Appl. Phys.* **39** 1001
[29] Pfeiffer L 1971 *J. Appl. Phys.* **42** 1725
[30] Hesse J, Graf T, Kopcewicz M, Afanas'ev A M and Chuev M A 1998 *Hyperfine Interact.* **113** 499
[31] Brown W F Jr 1963 *Phys. Rev.* **130** 1677
[32] Landau L D and Lifshitz E M 1935 *Phys. Z. Sowjetunion* **8** 153
[33] Gilbert T 1955 *Phys. Rev.* **100** 1243
[34] Schrefl T 1999 *J. Magn. Magn. Mater.* **207** 45
[35] Sun Z Z and Wang X R 2005 *Phys. Rev.* B **71** 174430
[36] Stoner E C and Wohlfarth E P 1948 *Phil. Trans. R. Soc.* A **240** 599
[37] Néel L 1949 *Ann. Géophys.* **5** 99
[38] Godovsky D Yu, Varfolomeev A V, Efremova G D, Cherepanov V M, Kapustin G A, Volkov A V and Moskvina M A 1999 *Adv. Mater. Opt. Electron.* **9** 87
[39] Hesse J and Rübartsch H 1974 *J. Phys. E: Sci. Instrum.* **7** 526
[40] Chuev M A, Hupe O, Bremers H, Hesse J and Afanas'ev A M 2000 *Hyperfine Interact.* **126** 407
[41] Afanas'ev A M and Chuev M A 2003 *JETP Lett.* **77** 415
[42] Afanas'ev A M and Chuev M A 2003 *J. Phys.: Condens. Matter* **15** 4827
[43] Mørup S 1994 *Hyperfine Interact.* **90** 171
[44] Chuev M A 2008 *JETP Lett.* **87** 707
[45] Anderson P W 1954 *J. Phys. Soc. Japan* **9** 316
[46] Afanas'ev A M, Chuev M A and Hesse J 1998 *JETP* **86** 983
[47] Chuev M A 2006 *JETP* **103** 243
[48] Zwanzig R 1964 *Physica* **30** 1109
[49] Dormann J L, Bessais L and Fiorani D 1988 *J. Phys. C: Solid State Phys.* **21** 2015
[50] Mørup S and Tronc E 1994 *Phys. Rev. Lett.* **72** 3278
[51] Hansen M F and Mørup S 1998 *J. Magn. Magn. Mater.* **184** 262
[52] Dormann J L, Fiorani D and Tronc E 1999 *J. Magn. Magn. Mater.* **202** 251
[53] Afanas'ev A M and Chuev M A 2001 *JETP Lett.* **74** 107
[54] Langevin P 1905 *J. Physique* **4** 678
[55] Bean C P 1955 *J. Appl. Phys.* **26** 1381
[56] Chuev M A 2009 *JETP* **135** at press